npg

Changes in subcellular localisation of MI-ER1α, a novel oestrogen receptor-α interacting protein, is associated with breast cancer progression

PL McCarthy[1], FC Mercer[1], MWJ Savicky[1], BA Carter[2], GD Paterno[1] and LL Gillespie*,[1]

[1]Division of BioMedical Sciences, Faculty of Medicine, Terry Fox Cancer Research Laboratories, Memorial University of Newfoundland, St John's, NL A1B 3V6, Canada; [2]Department of Pathology and Laboratory Medicine, Faculty of Medicine, Memorial University of Newfoundland, St John's, NL A1B 3V6, Canada

The oestrogen receptor-α (ERα) plays a key role in breast development and tumorigenesis and inhibiting its activity remains a prime strategy in the treatment of ERα-positive breast cancers. Thus, elucidation of the molecular mechanisms responsible for regulating ERα activity may facilitate the design of new, more effective breast cancer therapies. The MI-ER1α is a novel transcriptional repressor that contains an LXXLL motif for interaction with nuclear hormone receptors. We investigated the ability of MI-ER1α to bind to ERα in HEK293 and MCF-7 breast carcinoma cells, using co-immunoprecipitation assays. In both cell lines, MI-ER1α interacted with ERα in the presence and absence of oestrogen, but the interaction was stronger in the absence of ligand. Functional analysis revealed that overexpression of MI-ER1α in T47D breast carcinoma cells results in inhibition of oestrogen-stimulated anchorage-independent growth, suggesting that MI-ER1α may play a role in regulating breast carcinoma cell proliferation *in vivo*. To explore this further, we performed an immunohistochemical analysis of normal breast tissue and breast carcinoma; a total of 110 cases were examined in whole tissue sections and 771 cases were analysed in tissue microarrays. No consistent difference in the MI-ER1α expression level between normal breast tissue and breast carcinoma was discernible. However, there was a dramatic shift in the subcellular localisation: nuclear MI-ER1α was detectable in 75% of normal breast samples and in 77% of hyperplasia, but in breast carcinoma, only 51% of DCIS, 25% of ILC and 4% of IDC contained nuclear staining. This shift from nuclear to cytoplasmic localisation of MI-ER1α during breast cancer progression suggests that loss of nuclear MI-ER1α might contribute to the development of invasive breast carcinoma.
British Journal of Cancer (2008) **99,** 639–646. doi:10.1038/sj.bjc.6604518   www.bjcancer.com
Published online 29 July 2008
© 2008 Cancer Research UK

Keywords: nuclear localisation; MI-ER1; oestrogen receptor; LXXLL motif; breast carcinoma; immunohistochemistry

Steroid hormones, in particular oestrogens and progesterones, are crucial not only for normal growth and development of the mammary gland, but also as growth factors for the large majority of mammary carcinomas (Anderson, 2002; Clarke *et al*, 2004). Indeed, ERα status of breast tumours provides a powerful prognostic and predictive indicator to guide treatment regimens. Moreover, therapies that target oestrogen synthesis (oopherectomy: aromatase inhibitors) and/or that block oestrogen action on its receptor are critical for the management of hormone-dependent breast cancers (Arnedos and Smith, 2007).

In the classic pathway, the cellular response to oestrogen is initiated by hormone binding to ERα (Clarke *et al*, 2004; Hall and McDonnell, 2005). This high-affinity binding leads to a conformational alteration of the receptor, nuclear translocation and homodimerisation of the receptor complex. These changes permit the ERα complexes to bind sequence-specific oestrogen response elements located in the regulatory regions of oestrogen target genes, thus controlling their level of transcription. As with any biological pathway, this simple scheme is influenced by additional regulatory mechanisms in the cell (Ascenzi *et al*, 2006). These include phosphorylation of ERα, crosstalk with other signal transduction pathways, interactions with alternate receptor isoforms, like ERβ, and binding of ERα to coactivator and corepressor proteins, all of which can influence the cell's transcriptional response to oestrogen. It is now clear that tumour growth in response to oestrogen and to anti-oestrogen therapies will depend upon the sum total of regulatory effects acting on ERα. Thus, understanding the molecular mechanisms involved in controlling ERα activity in tumour cells will not only be critical for the development of new markers for screening and early detection, but also for the identification of additional prognostic indicators for treatment design and novel targets for the development of more effective breast cancer therapies.

Mesoderm induction early response 1 is a novel, highly conserved transcriptional regulator (Paterno *et al*, 1997, 1998; Thorne *et al*, 2005) discovered during a screen for fibroblast growth factor response genes (Paterno *et al*, 1997). The MI-ER1 protein includes several domains common to transcriptional regulators: the N terminus contains four acidic stretches that function as an acidic activation domain (Paterno *et al*, 1997).

Immediately downstream is an ELM2 domain, followed by a SANT motif; the ELM2 domain is involved in recruitment of histone deacetylase (HDAC) activity, which leads to changes in chromatin structure and results in transcriptional repression (Ding et al, 2003). Likewise, the MI-ER1 SANT domain functions in gene repression by interacting with Sp1 and interfering with its ability to bind to its cognate site on responsive promoters (Ding et al, 2004). Thus, MI-ER1 has the ability to function as both activator and repressor of gene transcription, depending on the cellular context.

Characterisation of the human mi-er1 gene revealed that there are two major protein isoforms, MI-ER1α and MI-ER1β, which differ in their C-terminal sequence (Paterno et al, 2002). Of particular interest is MI-ER1α, as it contains in its C terminus a consensus LXXLL interaction domain characteristic of nuclear hormone receptor (NR) coregulators. Initial expression analysis indicated that mi-er1 mRNA was differentially expressed in breast carcinoma cell lines and breast tumours (Paterno et al, 1998); however this study did not distinguish between the two MI-ER1 isoforms. In the current report, we examined the ability of MI-ER1α to interact with ERα, its effect on oestrogen-stimulated growth and its expression pattern in normal human breast tissue and primary breast carcinoma.

MATERIALS AND METHODS

Cell lines, plasmids and transfections

The cell lines MCF-7 and HEK293 were obtained from the American Tissue Culture Collection (Manassas, VA, USA); the T47D Tet-On cell line was purchased from Clontech (Mountain View, CA, USA). All cell lines were cultured according to the supplier's instructions. For oestrogen treatment, the media was replaced with phenol red-free media supplemented with 10% charcoal-stripped foetal bovine serum, 24 h before stimulation; 10 nM 17-β estradiol (E2) (Sigma) was added to the culture medium 3 h before harvesting.

The pCS3 + MT containing hmi-er1α (Genbank: NM_001077704) has been described elsewhere (Ding et al, 2003). pTRE-tight-hmi-er1α was generated by inserting a BamHI–XhoI fragment from pCS3 + MT-hmi-er1α into BamHI–SalI cut pTRE-tight vector (Clontech). The pcDNA3 vector containing hERα cDNA (Genbank: NM_00125) was a gift from Dr Christine Pratt (University of Ottawa). All plasmids were sequenced to verify the junctions and the MI-ER1α or hERα sequence.

All transfections were performed as previously described (Ding et al, 2003) in 6-well plates, using 1.6 μg of plasmid DNA. A total of 10^5 cells per well were seeded 18 h before transfection and cells were harvested after 48 h in culture.

Antibodies

The MI-ER1α antibody is a rabbit polyclonal antibody directed against a synthetic peptide representing alpha-specific sequence (amino acids 413–426); its production has been described and its specificity has been determined previously (Paterno et al, 2002; Thorne et al, 2008). Purified IgG was prepared from pre-immune or immune serum using the Melon Gel IgG purification kit (Pierce, Rockford, IL, USA) according to the manufacturer's instructions. Anti-ERα antibodies (D-12 and HC-20) were purchased from Santa Cruz Biotechnology Inc. (Santa Cruz, CA, USA).

Co-immunoprecipitation and Western blot analysis

For the co-immunoprecipitation (co-IP) assays, either 1×10^6 non-transfected MCF-7 cells or 2×10^5 HEK293 cells co-transfected with pcDNA3-erα and either pCS3 + MT or pCS3 + MT-mier1α were used per sample. Cells were lysed as shown by Ding et al (2003) and

subjected to immunoprecipitation and western blotting as shown by Ryan and Gillespie (1994). For determination of expression levels, cells were lysed directly into SDS–PAGE loading buffer and equivalent amounts of protein analysed by western blot as above.

Establishment of stably transfected T47D cell clones and doxycycline induction

Generation of MI-ER1α Tet-On T47D cell clones was done as described by Ding et al (2004), using a pTRE-tight-hmi-er1α construct. Control cell lines were generated by transfection with the pTRE-tight empty vector. Stable clones were induced to express MI-ER1α using 2 μg ml^{-1} doxycycline (dox) and expression was verified by western blot analysis of whole cell extracts, using our anti-MI-ER1α-specific antibody (Paterno et al, 2002).

Colony formation in soft agar

A total of 2×10^4 cells were plated in 0.35% agarose on a layer of 0.5% agarose, prepared $\pm 2 \mu g\, ml^{-1}$ dox, $\pm 10\, nM$ E2; controls included the equivalent volume of buffer and/or ethanol. Media, dox and E2 were replenished every 4 days and colonies were stained with crystal violet after 18 days and counted.
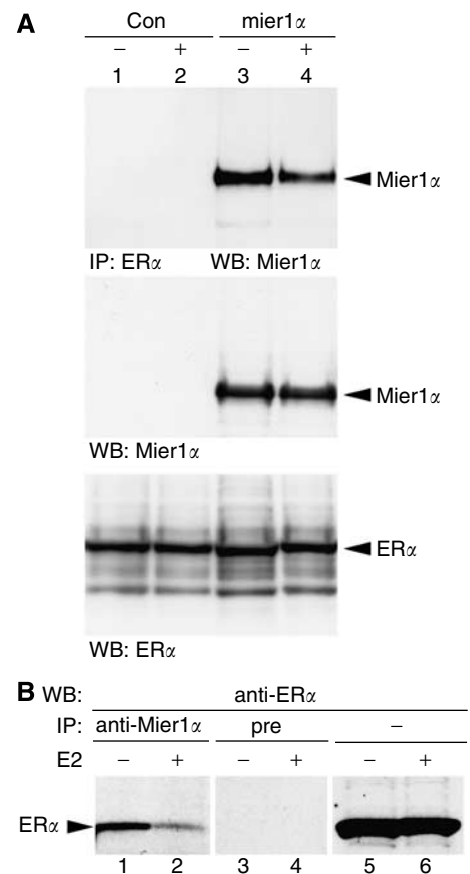

Figure 1 MI-ER1α interacts with ERα in vivo. (**A**) HEK293 cells were transfected with pcDNA3-herα and either pCS3 + MT-mier1α (lanes 3 and 4) or control empty vector (lanes 1 and 2) and treated with vehicle (lanes 1 and 3) or 10 nM E2 (lanes 2 and 4) for 3 h before extraction. Extracts were subjected to immunoprecipitation with anti-ERα (top panel) or loaded directly onto the gel (middle and bottom panels). Western blots were stained for MI-ER1α (top and middle panels) or ERα (bottom panel). (**B**) Extracts from MCF-7 cells treated with vehicle (lanes 1, 3 and 5) or 10 nM E2 (lanes 2, 4 and 6) were subjected to IP with anti-mier1α (lanes 1 and 2), pre-immune (lanes 3 and 4) or loaded directly onto the gel (lanes 5 and 6); Western blotting was performed with anti-ERα.

Study subjects

This study was approved by the Human Investigations Committee at Memorial University (HIC approval no. 05.56). One hundred and ten cases of primary invasive ductal carcinoma were identified from the database of the NL Eastern Health Cancer Registry for the years 2005 and 2006. Hematoxylin-and–eosin-stained slides for each case were reviewed by a pathologist (B. Carter) and all well-fixed tumour samples that contained adjacent normal ductal epithelium were selected for this study. One formalin-fixed, paraffin-embedded tissue block from each case was retrieved from the archives of the Department of Pathology and Laboratory Medicine, Memorial University, upon approval from Eastern Health's Medical Advisory and Board of Trustees Research Proposal Approval Committee.

Tissue microarrays, whole tissue sections and immunohistochemistry

The MI-ER1α protein expression pattern was examined both in TMAs and in whole tissue sections. The tissue microarrays (TMAs) enabled us to compare a large number of samples under identical staining conditions, whereas whole tissue sections allowed us to examine larger areas of tumour and normal tissue from a single sample.

Sections of human adrenal gland and small intestine were purchased from US Biomax Inc. (Rockville, MD, USA). Microarrays were purchased from US Biomax Inc., Biochain (Hayward, CA, USA) and the Cooperative Human Tissue Network (http://chtn.nci.nih.gov). Fourteen different TMAs containing a total of 204 normal, 91 hyperplasia, 78 DCIS, 102 ILC and 343 IDC samples were stained. Any cores that were of questionable pathology were reviewed by a pathologist. Some of the samples could not be assessed as either the core was missing or contained insufficient relevant tissue. The number of cases that were scored in each category is listed in the Results section.

Immunohistochemistry and preabsorption with peptide was performed as described previously (Thorne *et al*, 2008) using the Universal LSAB$^+$-HRP kit (Dako, Denmark) and 1.25 μg ml^{-1} of anti-MI-ER1α IgG or pre-immune IgG. Antigen retrieval was performed in 10 mM sodium citrate, pH 6.0, in a 95 °C water bath. Optimum retrieval time was determined empirically to be 40 min for whole tissue sections and 30 min for TMAs. As a control, each batch included slides stained with pre-immune IgG. Each sample was evaluated for staining using the Allred scoring system (Allred *et al*, 1993; Harvey *et al*, 1999), which consists of a combined score for staining intensity (0 = no, 1 = weak, 2 = moderate and 3 = intense staining) and proportion of positive cells (0 = 0, 1 = <1/100, 2 = 1/100–1/10, 3 = 1/10–1/3, 4 = 1/3–2/3, 5 = >2/3 stained). The sum of the two produces an Allred score; the value for the tumour cells was compared with that of normal adjacent tissue. For the assessment of nuclear staining, samples were scored positive if at least 5% of the nuclei in the section were stained; however, the majority of normal samples that scored positive contained at least 50% positive nuclei, whereas the majority of positive tumour samples contained fewer than 10% positive nuclei.

Statistical analysis

Correlation between the relative intensity of MI-ER1α staining in tumour sections and various clinicopathological parameters was subjected to χ^2 analysis (Pearson's test, two-tailed, 95% confidence interval) using SPSS v.13.0 software. The percentage of nuclear staining in the carcinoma samples was compared with that in normal breast tissue using a two-sided Fisher's exact test and the InStat v.3.0 software program (GraphPad Software, San Diego, CA, USA).

RESULTS

MI-ER1α interacts with ERα *in vivo*

We investigated the ability of MI-ER1α to physically associate with ERα in HEK293 cells transfected with *mi-er1α* and *erα*, using co-IP

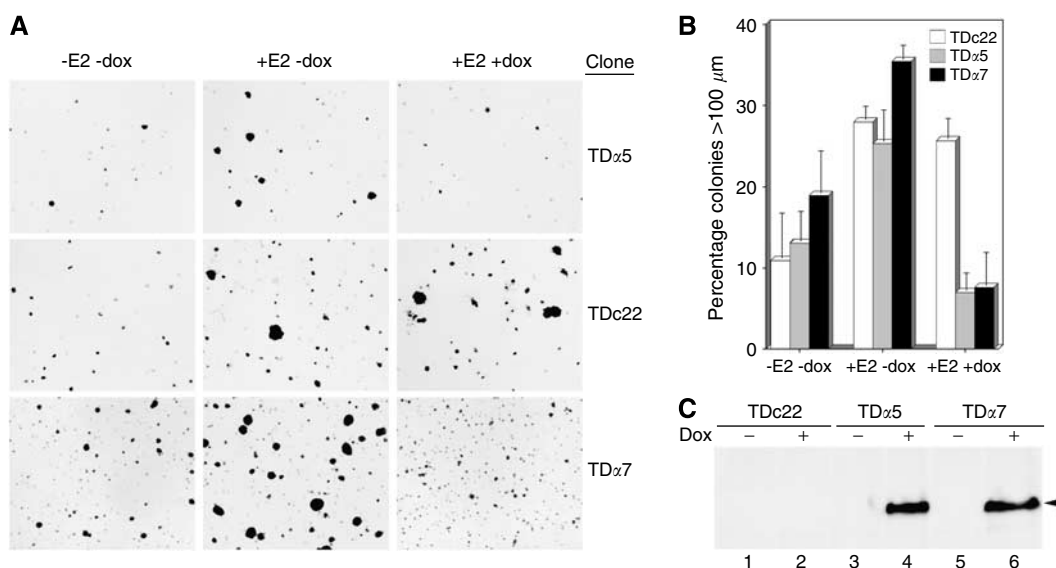**Figure 2** Overexpression of MI-ER1α reduces anchorage-independent growth of T47D breast carcinoma cells. Control (TDc22)- or MI-ER1α (TDα5 and TDα7)-expressing Tet-On T47D clones were cultured in 0.35% agarose, in the presence or absence of 2 μg ml^{-1} dox and in the presence or absence of 10 nM E2, as described in the Materials and methods. Colonies were stained with crystal violet, and colony size was measured using an ocular micrometre. A minimum of six fields from each plate was analysed; the number of colonies larger than 100 μm in size, expressed as a percentage of the total number of colonies, was recorded for each treatment. (**A**) Representative fields for each treatment combination for each clone are shown. (**B**) Histogram showing the average values and error bars for three independent experiments, performed in duplicate. (**C**) Western blot analysis to verify dox-specific induction of MI-ER1α expression. A representative blot of extracts from TDc22, TDα5 and TDα7 cells, cultured in the absence (lanes 1, 3 and 5) or presence (lanes 2, 4 and 6) of 2 μg ml^{-1} dox, is shown. The position of MI-ER1α is indicated.

assays. Our results show that ERα co-immunoprecipitates with MI-ER1α both in the presence and absence of ligand (E2); however, the intensity of the interaction was slightly reduced in the presence of ligand (Figure 1A). This difference was not due to variability in the expression levels of MI-ER1α or ERα, as these remained constant (Figure 1A).

To verify that endogenous MI-ER1α interacts with endogenous ERα, co-IP analysis of extracts from an ER + breast carcinoma cell line, MCF-7, was performed using our anti-MI-ER1α antibody. As can be seen in Figure 1B, ERα was detected in the MI-ER1α immunoprecipitate (lanes 1 and 2), but not in the pre-immune immunoprecipitate (lanes 3 and 4), demonstrating a specific interaction between MI-ER1α and ERα. As seen in the HEK293 cells, this interaction was stronger in the absence of E2 (Figure 1B, lanes 1 and 2). These results demonstrate that endogenous complexes containing MI-ER1α and ERα exist in the cell.

MI-ER1α reduces E2-stimulated growth of ER + breast carcinoma cells

To investigate the functional effect of MI-ER1α-ERα interaction on cellular responses to E2, we produced dox-inducible MI-ERα T47D clonal cell lines. Control (TDc22) and MI-ER1α-expressing (TDα5 and TDα7) clones were assessed for their ability to proliferate in soft agar, when stimulated by E2. In the absence of dox, E2 stimulated the growth of both control and MI-ER1α clones, as measured by the increase in colony diameter (Figure 2A and B). However, induction of MI-ER1α expression by exposure to 2 μg ml^{-1} dox dramatically reduced the ability of E2 to stimulate colony growth, although having no effect on the growth of TDc22 control cells (Figure 2A and B). Dox induction of MI-ER1α expression in the clones was verified by western blot analysis (Figure 2C). These results demonstrate that MI-ER1α reduces E2-stimulated anchorage-independent growth of breast carcinoma cells.
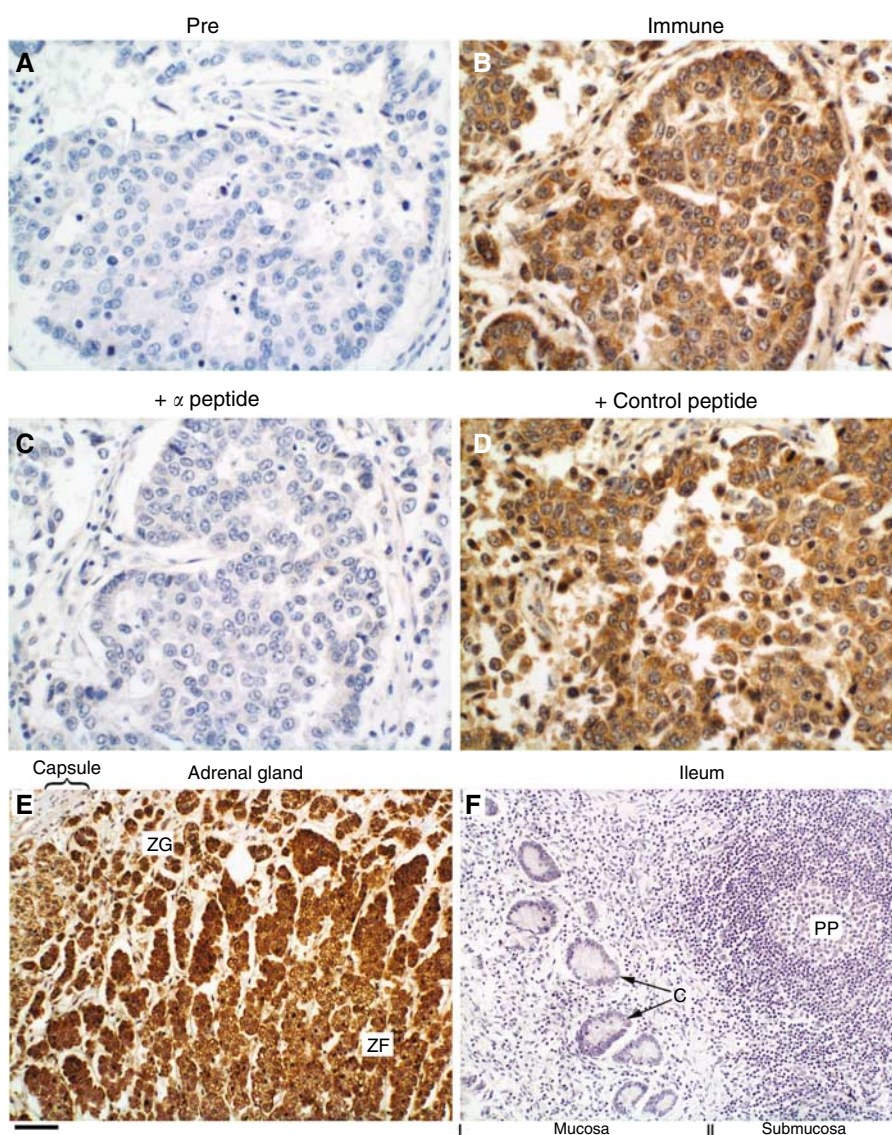
Figure 3 Immunohistochemical staining with anti-MI-ER1α. Human breast tumour sections were stained with pre-immune IgG (**A**), anti-mier1α IgG (**B**) or anti-mier1α IgG that had been pre-incubated with the α-specific peptide (**C**) or a control peptide (**D**). Note that only the peptide used to generate the antibody blocks staining. Sections of normal human adrenal gland (**E**) and normal human small intestine (**F**) stained with anti-mier1α IgG served as positive and negative tissue controls, respectively. Panel **E** shows a portion of the adrenal cortex that includes part of the zona glomerulosa (ZG) and zona fasciculata (ZF), whereas Panel **F** shows a section through the ileum that includes lymphoid tissue (Peyer's patch (PP)) and crypts of Lieberkühn (**C**). Scale bar = 50 μm for **A**–**D** and 100 μm for **E** and **F**.

Immunohistochemical analysis of MI-ER1α in normal breast and breast carcinoma

The MI-ER1α antibody used in this study has been well characterised and shown to be specific for the MI-ER1α protein (Paterno et al, 2002; Thorne et al, 2008). For this study, we used purified anti-MI-ER1α IgG and performed initial tests to confirm the specificity of antibody staining on paraffin sections of human tissue. Sections of breast tumours were stained in parallel with pre-immune IgG (Figure 3A), anti-MI-ER1α IgG (Figure 3B), anti-MI-ER1α IgG, which had been preabsorbed with the α-peptide used to generate the antibody (Figure 3C) or with an unrelated peptide (control peptide; Figure 3D). As can be seen in Figure 3, preabsorption of the antibody with the α-peptide blocked staining and produced results very similar to that obtained with pre-immune IgG. The control peptide, on the other hand, did not affect antibody binding, and the staining was similar to that obtained with the anti-MI-ER1α IgG alone. Additional positive and negative controls included sections of normal human adrenal cortex and small intestine, respectively; previously, we reported positive staining in the murine adrenal gland, whereas most areas of the small intestine were negative (Thorne et al, 2008). As can be seen in Figure 3E and F, staining of the human tissues was similar to that seen in the mouse, with intense staining of the adrenal cortex and no immunoreactivity in the ileum.

Of the TMAs used in this study, the cores that contained sufficient tissue for assessment included 180 cases of normal breast, 81 hyperplasia, 71 DCIS, 325 IDC and 99 ILC. In addition, there were 16 cores containing lymph node metastases. An additional 85 cases of IDC and adjacent normal breast tissue were examined in whole tissue sections.

First, we determined the MI-ER1α expression pattern. In normal breast tissue, staining was observed primarily in the ductal epithelial cells (Figure 4G–I); there was some weaker staining of vascular endothelial cells (inset in Figure 4H) but very little or no staining of the stroma. Some variability was observed in the intensity of staining of the ductal epithelium and no obvious difference in staining intensity of the ducts vs the lobules. In the
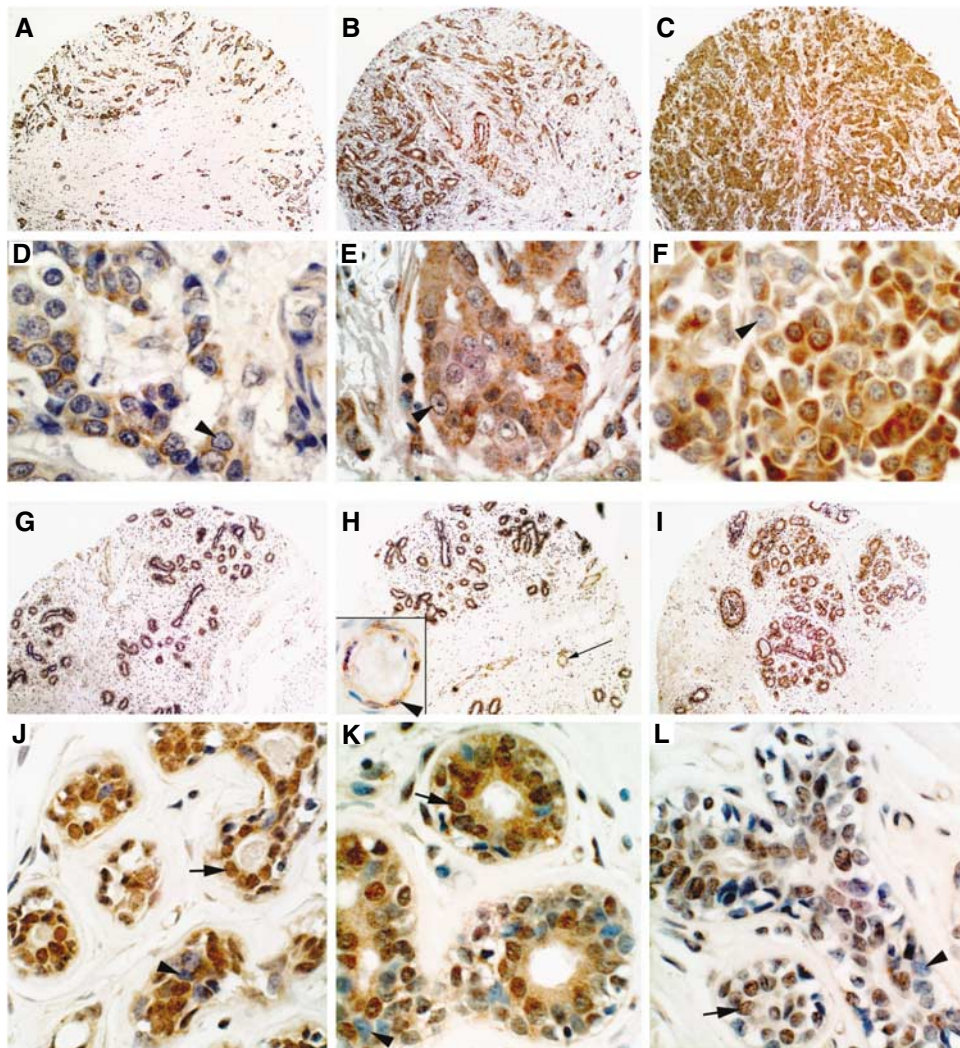

Figure 4 Expression pattern of MI-ER1α in normal breast tissue and invasive ductal carcinoma. (**A**–**C**) Low magnification of representative examples of primary invasive ductal carcinoma. (**D**–**F**) High magnification of IDC illustrating the subcellular localisation of MI-ER1α. Note that the nuclei (arrowheads) are negative (blue) and that MI-ER1α expression (brown) is exclusively cytoplasmic. (**G**–**I**) Low magnification of representative examples of normal breast tissue. MI-ER1α expression is detected primarily in the ducts with little or no expression in the surrounding stroma. The inset in H shows a higher magnification of the blood vessel indicated by a long arrow and illustrates weak staining of endothelial cells (arrowhead). (**J**–**L**) High magnification of normal ducts. Arrows indicate nuclear MI-ER1α staining; arrowheads indicate examples of negative nuclei. Scale bar = 250 μm for **A**–**C** and **G**–**I**, 25 μm for **D**–**F**, **J**–**L** and inset in **H**.

Molecular Diagnostics

tumours, the staining pattern was similar to that in normal tissue, with expression in the tumour cells themselves and little or no staining of the stroma (Figure 4A–C).

Next, staining in whole tissue sections was assessed using the Allred scoring system, which consists of a combined score for intensity level (0–3) and proportion of positive cells (0–5). The Allred score for the tumour was compared with that for adjacent normal tissue. Overall, there was no consistent difference in scores between the tumour and adjacent normal tissue, that is, some tumours had lower values than adjacent normal, some had higher values and some had equal values. These three categories of relative Allred scores were analysed for correlation with a number of clinical parameters, which included patient age, tumour size, lymph node status, grade (modified Scarff–Bloom–Richardson), stage (TNM), ER, PR and Her2/neu status (Table 1). No statistically significant correlation was found, as determined by χ^2 analysis (Table 1). In addition, we analysed the intensity and proportion scores separately and found no statistically significant correlation (data not shown).

Samples were also examined for the subcellular localisation of MI-ER1α and initially scored as nuclear only, cytoplasmic only or nuclear and cytoplasmic. As virtually all samples had some cytoplasmic staining but the presence of nuclear staining was limited, samples were then separated into two categories: nuclear

Table 1 Analysis of correlation between clinicopathological parameters and relative MIER1α staining in breast carcinoma

Parameters	MIER1 expression:[a] tumor Allred score vs normal Allred score			Total	P-value[b]
	Less than normal	Equal to normal	Greater than normal		
Age					
<50	6 (19.4)	4 (12.9)	21 (67.7)	**31**	
>=50	8 (10.1)	16 (20.3)	55 (69.6)	**79**	P = 0.410
Age					
<=44	5 (25.0)	3 (15.0)	12 (60.0)	**20**	
44–64	4 (7.5)	9 (17.0)	40 (75.5)	**53**	
>=65	5 (13.9)	8 (19.4)	24 (66.7)	**37**	P = 0.365
Tumor size (TNM)					
T1	6 (10.2)	11 (18.6)	42 (71.2)	**59**	
T2	7 (16.7)	6 (14.3)	29 (69.0)	**42**	
T3 and T4	1 (11.1)	3 (33.3)	5 (55.6)	**9**	P = 0.618
Tumor size (categorical)					
<=2 cm	6 (10.2)	11 (18.6)	42 (71.2)	**59**	
>2 cm	8 (15.7)	9 (17.6)	34 (66.7)	**51**	P = 0.693
Lymph node involvement					
No	6 (13.6)	9 (20.5)	28 (63.6)	**43**	
Yes	4 (12.5)	6 (18.8)	22 (68.8)	**32**	P = 0.957
Lymph node status (TNM)					
N0	6 (13.6)	9 (20.5)	28 (63.6)	**43**	
N1	4 (16.0)	5 (20.0)	16 (64.0)	**25**	
N2	0 (0)	0 (0)	6 (100.0)	**6**	
N3	0 (0)	0 (0)	1 (100.0)	**1**	P = 0.941
Grade[c]					
1	6 (20.0)	8 (26.7)	16 (53.3)	**30**	
2	5 (11.9)	8 (19.1)	29 (69.0)	**42**	
3	3 (8.1)	4 (10.8)	30 (81.1)	**37**	P = 0.217
Stage[d]					
I	1 (4.0)	6 (24.0)	18 (72.0)	**25**	
II	9 (23.1)	4 (10.3)	26 (66.6)	**39**	
III	0 (0)	3 (27.3)	8 (72.7)	**11**	
IV	0	0	0	**0**	P = 0.082
ER					
Negative	2 (12.5)	2 (12.5)	12 (75.0)	**16**	
Positive	10 (11.2)	16 (18.0)	63 (70.8)	**89**	P = 0.891
PR					
Negative	3 (10.8)	2 (7.1)	23 (82.1)	**28**	
Positive	9 (11.8)	15 (19.7)	52 (68.4)	**76**	P = 0.300
HER2/neu status					
Negative	10 (13.5)	15 (20.3)	49 (66.2)	**74**	
Positive	1 (6.7)	0 (0)	14 (93.3)	**15**	P = 0.086

[a]Values are listed as number of subjects, with percentage listed in brackets. [b]P-value; χ^2 analysis (Pearson's test, two-tailed, 95% CI), statistical significance is assumed when $P < 0.05$. [c]Modified Scarff–Bloom–Richardson grading system. [d]FIGO staging system.
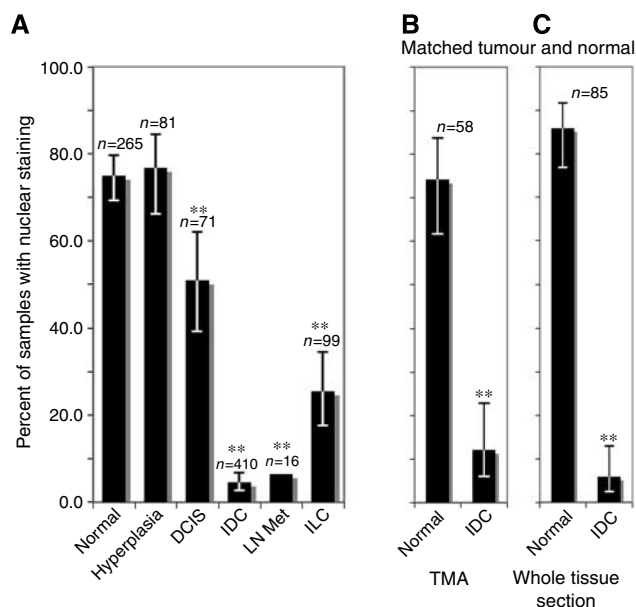
Figure 5 Loss of nuclear MI-ER1α during breast cancer progression. (**A**) Values from TMAs and whole tissue sections. The percentages and 95% confidence intervals are shown. The number of samples (*n*) in each category is listed above the bar; ** indicates $P \leqslant 0.0001$. (**B**) Values from TMAs containing a total of 58 matched normal and IDC samples. (**C**) Values from whole tissue sections; 85 samples containing matched IDC and normal adjacent tissue were analysed.

staining and no nuclear staining. The results were quite striking, showing a large differential between the percentage of normal tissue samples and IDC that were positive for nuclear staining: 74.7 *vs* 4.4%, respectively ($P < 0.0001$; Figures 4D–F, 4J–L, 5A). In addition, the proportion of stained nuclei within a sample was different: most tumour samples that displayed nuclear MI-ER1α contained fewer than 10% stained nuclei, whereas the majority of normal samples contained > 50% stained nuclei. A differential in nuclear staining between normal and ILC was observed as well (74.7 *vs* 25.3%; $P < 0.0001$; Figure 4A). We examined nuclear staining in other subtypes, namely hyperplasia and DCIS. The percentage nuclear staining in hyperplasia was similar to that of normal samples (76.5%; $P = 0.8831$; Figure 5A), whereas DCIS was intermediate between normal and IDC (50.7%; $P = 0.0001$; Figure 5A). Cases of lymph node metastases from patients with IDC showed levels of nuclear staining similar to IDC (6.3%; $P = 0.5009$; Figure 5A).

It was important to compare nuclear staining in tumour samples with adjacent normal tissue from the same patient, to ensure that the observed difference in MI-ER1α subcellular localisation is not merely due to individual patient differences. Therefore, we analysed 58 cases from TMAs that contained matched tumour–normal cores (Figure 5B); in addition, we compared tumour and normal adjacent areas in whole tissue sections from 85 cases of IDC (Figure 5C). Both gave results similar to that described above: the majority of tumours lacked nuclear staining, whereas most of the adjacent normal areas showed nuclear staining (Figure 5B and C). Together, these data demonstrate that a shift in the subcellular localisation of MI-ER1α is associated with breast cancer progression.

DISCUSSION

Our demonstration that MI-ER1α can physically interact with ERα and that regulated overexpression of MI-ER1α dramatically affects

oestrogen-stimulated growth of breast carcinoma cells indicates that MI-ER1α functions as an ER corepressor. A number of ERα corepressors have been identified (Hall and McDonnell, 2005) and MI-ER1 is similar in structure and function to other known NR corepressors, including NCoR (Horlein *et al*, 1995), SMRT (Chen and Evans, 1995) and MTA1–3 (Manavathi and Kumar, 2007), which also recruit HDAC activity to repress transcription.

Traditionally, corepressors bind unliganded NRs, whereas coactivators bind liganded NRs; however, ERα is distinct from other NRs in this regard (Dobrzycka *et al*, 2003). For example, the classic corepressors, NCoR (Horlein *et al*, 1995) and SMRT (Chen and Evans, 1995), interact only with antagonist-bound ERα, whereas LCoR interacts with ERα only in the presence of oestrogen (Fernandes *et al*, 2003). Our results show that MI-ER1α binds ERα in the presence and absence of oestrogen and, in this regard, is similar to BRCA1, which regulates both oestrogen-stimulated and unliganded ERα activity (Fan *et al*, 2001; Rosen *et al*, 2005).

Previously, we reported a PCR analysis that demonstrated a significant increase in *mi-er1* mRNA expression levels in breast tumours when compared with normal breast tissue (Paterno *et al*, 1998). However, our current study shows no consistent difference in MI-ER1α protein expression levels. This discrepancy is most likely due to the fact that MI-ER1α expression in normal tissue is restricted primarily to ductal epithelial cells, whereas within the tumour, virtually all tumour cells are positive for MI-ER1α. Thus, the proportion of cells expressing *mi-er1* mRNA per volume of tissue would be much lower in normal breast than in a solid tumour sample.

Our immunohistochemical analysis showed that although virtually all (96%) IDC samples have lost nuclear MI-ER1α, only half of the DCIS samples showed this shift in subcellular localisation. Ductal carcinoma *in situ* consists of a heterogeneous group of pre-invasive lesions that may or may not progress to IDC and, at the moment, it is not possible to accurately predict which patients are at risk (Wiechmann and Kuerer, 2008). Thus, it will be important to determine the value of MI-ER1α as a prognostic indicator, using a larger sample size. A key question is whether loss of nuclear MI-ER1α is associated with specific subtypes of DCIS or any other parameter correlated with progression to IDC. Such parameters include histological criteria, for example, nuclear grade and cell necrosis, as well as molecular markers, for example, loss of IGFBP-rP1 expression (Wiechmann and Kuerer, 2008). As more prognostic markers are identified, it may become possible to define a molecular-histological fingerprint for DCIS that can accurately predict a patient's risk of recurrence as invasive carcinoma.

Our observations in this study are consistent with a model where, in the progression to IDC, MI-ER1α is shuttled to the cytoplasm such that it cannot exert its gene/chromatin repressor functions. This may include loss of the functional interaction between MI-ER1α and ERα. Alternatively, it may act in a manner similar to MTA1s, a splicing isoform of MTA1, which binds to ERα in the cytoplasm and enhances ERα non-genomic activities, including stimulation of peptide growth factor signal transduction pathways (Kumar *et al*, 2002). The net result is an increase in breast carcinoma cell proliferation. We are currently investigating the molecular mechanisms of MI-ER1α localisation in breast cancer cells and its role in tumour progression to an invasive phenotype.

Molecular Diagnostics

REFERENCES

Allred DC, Clark GM, Elledge R, Fuqua SA, Brown RW, Chamness GC, Osborne CK, McGuire WL (1993) Association of p53 protein expression with tumor cell proliferation rate and clinical outcome in node-negative breast cancer. *J Natl Cancer Instit* **85:** 200–206

Anderson E (2002) The role of oestrogen and progesterone receptors in human mammary development and tumorigenesis. *Breast Cancer Res* **4:** 197–201

Arnedos M, Smith I (2007) Progression of endocrine therapies for breast cancer: where are we headed? *Expert Rev Anticancer Ther* **7:** 1651–1664

Ascenzi P, Bocedi A, Marino M (2006) Structure–function relationship of estrogen receptor alpha and beta: impact on human health. *Mol Aspects Med* **27:** 299–402

Chen JD, Evans RM (1995) A transcriptional co-repressor that interacts with nuclear hormone receptors. *Nature* **377:** 454–457

Clarke RB, Anderson E, Howell A (2004) Steroid receptors in human breast cancer. *Trends Endocrinol Metabol* **15:** 316–323

Ding Z, Gillespie LL, Mercer FC, Paterno GD (2004) The SANT domain of human MI-ER1 interacts with Sp1 to interfere with GC box recognition and repress transcription from its own promoter. *J Biol Chem* **279:** 28009–28016

Ding Z, Gillespie LL, Paterno GD (2003) Human MI-ER1 alpha and beta function as transcriptional repressors by recruitment of histone deacetylase 1 to their conserved ELM2 domain. *Mol Cell Biol* **23:** 250–258

Dobrzycka KM, Townson SM, Jiang S, Oesterreich S (2003) Estrogen receptor corepressors – a role in human breast cancer? *Endocr Relat Cancer* **10:** 517–536

Fan S, Ma YX, Wang C, Yuan RQ, Meng Q, Wang JA, Erdos M, Goldberg ID, Webb P, Kushner PJ, Pestell RG, Rosen EM (2001) Role of direct interaction in BRCA1 inhibition of estrogen receptor activity. *Oncogene* **20:** 77–87

Fernandes I, Bastien Y, Wai T, Nygard K, Lin R, Cormier O, Lee HS, Eng F, Bertos NR, Pelletier N, Mader S, Han VK, Yang XJ, White JH (2003) Ligand-dependent nuclear receptor corepressor LCoR functions by histone deacetylase-dependent and -independent mechanisms. *Mol Cell* **11:** 139–150

Hall JM, McDonnell DP (2005) Coregulators in nuclear estrogen receptor action: from concept to therapeutic targeting. *Mol Interv* **5:** 343–357

Harvey JM, Clark GM, Osborne CK, Allred DC (1999) Estrogen receptor status by immunohistochemistry is superior to the ligand-binding assay for predicting response to adjuvant endocrine therapy in breast cancer. *J Clin Oncol* **17:** 1474–1481

Horlein AJ, Naar AM, Heinzel T, Torchia J, Gloss B, Kurokawa R, Ryan A, Kamei Y, Soderstrom M, Glass CK, Rosenfeld MG (1995) Ligand-independent repression by the thyroid hormone receptor mediated by a nuclear receptor co-repressor. *Nature* **377:** 397–404

Kumar R, Wang R-A, Mazumdar A, Talukder AH, Mandal M, Yang Z, Bagheri-Yarmand R, Sahin A, Hortobagyi G, Adam L, Barnes CJ, Vadlamudi RK (2002) A naturally occurring MTA1 variant sequesters oestrogen receptor-[alpha] in the cytoplasm. *Nature* **418:** 654–657

Manavathi B, Kumar R (2007) Metastasis tumor antigens, an emerging family of multifaceted master coregulators. *J Biol Chem* **282:** 1529–1533

Paterno GD, Ding Z, Lew YY, Nash GW, Mercer FC, Gillespie LL (2002) Genomic organization of the human mi-er1 gene and characterization of alternatively spliced isoforms: regulated use of a facultative intron determines subcellular localization. *Gene* **295:** 79–88

Paterno GD, Li Y, Luchman HA, Ryan PJ, Gillespie LL (1997) cDNA cloning of a novel, developmentally regulated immediate early gene activated by fibroblast growth factor and encoding a nuclear protein. *J Biol Chem* **272:** 25591–25595

Paterno GD, Mercer FC, Chayter JJ, Yang X, Robb JD, Gillespie LL (1998) Molecular cloning of human er1 cDNA and its differential expression in breast tumours and tumour-derived cell lines. *Gene* **222:** 77–82

Rosen EM, Fan S, Isaacs C (2005) BRCA1 in hormonal carcinogenesis: basic and clinical research. *Endocr Relat Cancer* **12:** 533–548

Ryan PJ, Gillespie LL (1994) Phosphorylation of phospholipase C gamma 1 and its association with the FGF receptor is developmentally regulated and occurs during mesoderm induction in *Xenopus laevis*. *Dev Biol* **166:** 101–111

Thorne LB, Grant AL, Paterno GD, Gillespie LL (2005) Cloning and characterization of the mouse ortholog of mi-er1. *DNA Seq* **16:** 237–240

Thorne LB, McCarthy PL, Paterno GD, Gillespie LL (2008) Protein expression of the transcriptional regulator MI-ER1 alpha in adult mouse tissues. *J Mol Histol* **39:** 15–24

Wiechmann L, Kuerer HM (2008) The molecular journey from ductal carcinoma *in situ* to invasive breast cancer. *Cancer* **112:** 2130–2142

Molecular Diagnostics